Applied Mathematics Letters 60 (2016) 36–42

Contents lists available at ScienceDirect

Applied Mathematics Letters

www.elsevier.com/locate/aml

Near-field imaging with far-field data

Gang Bao[a], Peijun Li[b,*], Yuliang Wang[c]

[a] School of Mathematical Sciences, Zhejiang University, Hangzhou, 310027, China
[b] Department of Mathematics, Purdue University, West Lafayette, IN 47907, USA
[c] Department of Mathematics, Hong Kong Baptist University, Kowloon, Hong Kong

ARTICLE INFO

Article history:
Received 8 January 2016
Accepted 31 March 2016
Available online 11 April 2016

Keywords:
Inverse scattering
Diffractive grating
Super-resolution

ABSTRACT

Using the inverse diffractive grating problem as an example, we demonstrate how a super-resolution can be achieved stably by using far-field data. The idea is to place a slab of a homogeneous medium with a large index of refraction above the grating surface, and more propagating wave modes can be utilized from the far-field data which contributes to the reconstruction resolution.

1. Introduction

According to the Rayleigh criterion, there is a resolution limit to the sharpness of details that can be observed by conventional far-field optical microscopy, one half the wavelength, referred to as the diffraction limit [1]. The loss of the details is related to the non-radiative components of the field known as evanescent waves [2]. It is severely ill-posed to directly use the evanescent waves since the noise in the measurements will be amplified exponentially. Therefore, near-field data is of paramount importance to achieve super-resolution [3,4]. However, it might be cumbersome to measure the near-field data as a sophisticated control is needed for the probe when scanning samples.

We use the diffraction grating problem as an example to demonstrate how a super-resolution can be achieved stably by using the far-field data. The idea is to place a slab of a homogeneous medium with a large index of refraction above the grating surface. A particular function of the slab is to convert more propagating wave modes of the far-field data into the near-field. The approach avoids measuring the sensitive near-field data.

Scattering theory in periodic structures has many significant applications in optical industry. The scattering problems have been studied extensively for periodic structures [5–9,14,15]. This paper is built upon

* Corresponding author.
E-mail address: lipeijun@math.purdue.edu (P. Li).

http://dx.doi.org/10.1016/j.aml.2016.03.023
0893-9659/

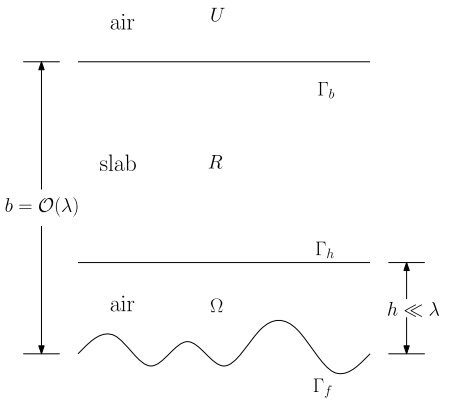

Fig. 1. Schematic of the problem geometry.

our recent work on solving a wide class of inverse surface scattering problems for acoustic, electromagnetic, and elastic waves [10–12], where the methods were designed especially for the near-field data. It reflects our effort to design more practical models and efficient methods for solving quantitatively complex inverse scattering problems with high resolution.

2. Problem formulation

Consider a perfect electrically conducting surface $\Gamma_f = \{(x, y) \in \mathbb{R}^2 : y = f(x), 0 < x < \Lambda\}$, where f is a periodic function with period Λ. The scattering surface function f is assumed to have the form

$$f(x) = \varepsilon g(x), \tag{2.1}$$

where $\varepsilon > 0$ is a sufficiently small constant g is also a periodic function with the same period Λ. Hence the surface Γ_f is a small perturbation of the planar surface $\Gamma_0 = \{(x, y) \in \mathbb{R}^2 : y = 0, 0 < x < \Lambda\}$.

Let a slab of a homogeneous dielectric medium be placed above Γ_f. The slab's bottom face is $\Gamma_h = \{(x, y) \in \mathbb{R}^2 : y = h, 0 < x < \Lambda\}$, where h, satisfying $\|f\|_\infty < h \ll \lambda$, is a positive constant. Here λ is the wavelength of the incident field. The slab's top face is $\Gamma_b = \{(x, y) \in \mathbb{R}^2 : y = b, 0 < x < \Lambda\}$, where b, satisfying $h \ll b = \mathcal{O}(\lambda)$, is also a positive constant.

Denote by Ω the bounded domain between Γ_f and Γ_h, i.e., $\Omega = \{(x, y) \in \mathbb{R}^2 : f < y < h, 0 < x < \Lambda\}$. Let R be the domain of the slab, i.e., $R = \{(x, y) \in \mathbb{R}^2 : h < y < b, 0 < x < \Lambda\}$. Denote by U the open domain above Γ_b, i.e., $U = \{(x, y) \in \mathbb{R}^2 : y > b, 0 < x < \Lambda\}$. The index of refraction is one in Ω and U since they are free spaces, and has a constant value $n > 1$ in the slab R. The schematic of the problem geometry is shown in Fig. 1.

Let an incoming plane wave $\phi^{\text{inc}}(x, y) = e^{-\mathrm{i}\kappa y}$ be normally incident on Γ_b from above, where κ is the free space wavenumber. Let ψ, ϕ, and φ be the diffracted field in U, the total field in R, and the total field in Ω, respectively. They satisfy the Helmholtz equations:

$$\begin{cases} \Delta\psi + \kappa^2\psi = 0 & \text{in } U, \\ \Delta\phi + (\kappa n)^2\phi = 0 & \text{in } R, \\ \Delta\varphi + \kappa^2\varphi = 0 & \text{in } \Omega, \end{cases} \tag{2.2}$$

and the boundary conditions:

$$\begin{cases} \varphi = 0 & \text{on } \Gamma_f, \\ \partial_y\psi = \mathscr{B}\psi & \text{on } \Gamma_b. \end{cases} \tag{2.3}$$

Here $\mathscr{B}$ is the boundary operator and is defined as follows:

$$(\mathscr{B}u)(x) = \sum_{m\in\mathbb{Z}} \mathrm{i}\beta_m u^{(m)} e^{\mathrm{i}\alpha_m x},$$

where $u^{(m)}$ is the Fourier coefficient of $u(x)$,

$$\alpha_m = m\left(\frac{2\pi}{\Lambda}\right), \quad \beta_m = \begin{cases} \left(\kappa^2 - \alpha_m^2\right)^{1/2}, & |\alpha_m| < \kappa, \\ \mathrm{i}\left(\alpha_m^2 - \kappa^2\right)^{1/2}, & |\alpha_m| > \kappa. \end{cases}$$

In addition, these wave fields are connected via the continuity conditions:

$$\begin{cases} \phi^{\mathrm{inc}} + \psi = \phi, \quad \partial_y\phi^{\mathrm{inc}} + \partial_y\psi = \partial_y\phi & \text{on } \Gamma_b, \\ \phi = \varphi, \quad \partial_y\phi = \partial_y\varphi & \text{on } \Gamma_h. \end{cases} \tag{2.4}$$

Given the incident field ϕ^{inc}, the inverse problem is to determine f from the far-field measurement of the total field ϕ on Γ_b, which is denoted by $\phi_b(x) = \phi(x, b)$. By far-field data, it means that the measurement distance b is comparable with the wavelength, i.e., $b = \mathcal{O}(\lambda)$.

3. Reduced problem

Consider the periodic solution of the Cauchy problem for ϕ in the slab R:

$$\begin{cases} \Delta\phi + (\kappa n)^2\phi = 0 & \text{in } R, \\ \phi = \phi_b & \text{on } \Gamma_b, \\ \partial_y\phi = \mathscr{B}\phi + \rho & \text{on } \Gamma_b, \end{cases} \tag{3.5}$$

where $\rho = -2\mathrm{i}\kappa e^{-\mathrm{i}\kappa b}$. It can be verified that the problem (3.5) has a unique solution which gives the far-to-near data conversion formula:

$$\begin{aligned} \phi^{(m)}(h) = {} & (2\eta_m)^{-1}[(\eta_m + \beta_m)\phi_b^{(m)} - \mathrm{i}\rho^{(m)}]e^{-\mathrm{i}\eta_m(b-h)} \\ & + (2\eta_m)^{-1}[(\eta_m - \beta_m)\phi_b^{(m)} + \mathrm{i}\rho^{(m)}]e^{\mathrm{i}\eta_m(b-h)}, \end{aligned} \tag{3.6}$$

where $\phi_b^{(m)}$ is the Fourier coefficient of the far-field data $\phi_b(x)$ and

$$\eta_m = \begin{cases} \left((\kappa n)^2 - \alpha_m^2\right)^{1/2}, & |\alpha_m| < \kappa n, \\ \mathrm{i}\left(\alpha_m^2 - (\kappa n)^2\right)^{1/2}, & |\alpha_m| > \kappa n. \end{cases} \tag{3.7}$$

Based on (3.6) and (3.7), it is easy to make the following observations: it is well-posed to convert the far-field data for the Fourier modes satisfying $|\alpha_m| < \kappa n$ in the sense that a small variation in the far-field data will not lead to a large error in the near-field data; it is severely ill-posed to convert the far-field data for the Fourier modes satisfying $|\alpha_m| > \kappa n$ as a small variation in the far-field data will be exponentially amplified and lead to a huge error in the near-field data. Therefore it is only reliable to make the near-field data by converting the low frequency far-field data $\phi_b^{(m)}$ with $|\alpha_m| < \kappa n$. Noticing $n > 1$ in the slab, we are allowed to include more frequency modes than the case without the slab in the reconstruction of the surface, which contribute to a super-resolution.

Finally, we may consider the reduced boundary value problem for φ in Ω:

$$\begin{cases} \Delta\varphi + \kappa^2\varphi = 0 & \text{in } \Omega, \\ \varphi = 0 & \text{on } \Gamma_f, \\ \partial_y\varphi = \mathscr{B}\varphi + r & \text{on } \Gamma_h, \end{cases} \tag{3.8}$$

where $r(x)$ has Fourier coefficient:

$$r^{(m)} = \mathrm{i}(2\eta_m)^{-1}\kappa^2(n^2-1)\left[e^{-\mathrm{i}\eta_m(b-h)} - e^{\mathrm{i}\eta_m(b-h)}\right]\phi_b^{(m)} + (2\eta_m)^{-1}\left[(\eta_m-\beta_m)e^{-\mathrm{i}\eta_m(b-h)} + (\eta_m+\beta_m)e^{\mathrm{i}\eta_m(b-h)}\right]\rho^{(m)}.$$

The inverse problem is reformulated to determine $f(x)$ from the Fourier coefficients $\varphi^{(m)}(h) = \phi^{(m)}(h)$ for $m \in \mathbb{Z}$ with $|\alpha_m| < \kappa n$.

4. Reconstruction formula

Consider a power series solution of the boundary value problem (3.8) in terms of ε:

$$\varphi(x,y) = \varphi_0(x,y) + \varepsilon\varphi_1(x,y) + e(x,y), \tag{4.9}$$

where $e = \mathcal{O}(\varepsilon^2)$ denotes the remainder consisting of all the high order terms. Dropping the remainder and evaluating (4.9) at $y = h$ gives an approximation

$$\varphi(x,h) = \varphi_0(x,h) + \varepsilon\varphi_1(x,h),$$

which yields

$$\varphi^{(m)}(h) = \varphi_0^{(m)}(h) + \varepsilon\varphi_1^{(m)}(h). \tag{4.10}$$

Noting $f = \varepsilon g$, we obtain an infinite dimensional linear system of equations for the Fourier coefficients of the solution:

$$\sum_{m'\in\mathbb{Z}} S_{m,m'} f^{(m-m')} = \varphi^{(m)}(h) - \varphi_0^{(m)}(h), \tag{4.11}$$

where $\varphi_0^{(m)} = (2\mathrm{i}\beta_m)^{-1}e^{\mathrm{i}\beta_m h}(e^{\mathrm{i}\beta_m h} - e^{-\mathrm{i}\beta_m h})r^{(m)}$ and $S_{m,m'} = -r^{(m')}e^{\mathrm{i}(\beta_m+\beta_{m'})h}$.

To truncate (4.11) into a finite dimensional system and to suppress the exponential growth of the error in the data, we choose the cut-off frequency N such that $|\alpha_m| < n\kappa$ for all $|m| \le N$, i.e.,

$$N = \left\lfloor \frac{n\kappa\Lambda}{2\pi} \right\rfloor.$$

It is clear to note from the above equation that the index of refraction n plays a critical role for the reconstruction resolution. The bigger the n is, the higher the resolution is. By keeping only the Fourier coefficients of the solution in $[-N, N]$, we obtain the truncated equation

$$AF = B, \tag{4.12}$$

where A is the $(2N+1)\times(2N+1)$ matrix given by

$$A(m,m') = S_{m,m-m'},$$

and F, B are $(2N+1)$ column vectors given by

$$F(m) = f^{(m)}, \qquad B(m') = \varphi^{(m')}(h) - \varphi_0^{(m')}(h)$$

for $-N \le m, m' \le N$. It is easy to note that $S_{m,m'}$ contains unstable terms which exponentially amplify error for $|m'| > N$. Hence we regularize (4.12) by letting $A_{m,m'} = 0$ if $|m-m'| > N$. Let the solution of (4.12) be given by

$$F = A^{\dagger}B, \tag{4.13}$$

where $A^{\dagger}$ denotes the Moore–Penrose pseudo inverse of A. Finally, the scattering surface is reconstructed as

$$f = \mathrm{Re}\sum_{|m|\le N} F(m)e^{\mathrm{i}\alpha_m x}. \tag{4.14}$$

5. Nonlinear correction scheme

The explicit inversion formula (4.14) is accurate to reconstruct the surface function for sufficiently small ε. If ε is not small, the reconstruction formula (4.14) may provide an initial approximation. To improve the reconstruction accuracy, we propose a nonlinear correction scheme.

Let F_0 be the reconstructed Fourier coefficients by (4.13) and f_0 be the reconstructed surface function by (4.14). Using f_0 as the surface function, we solve the direct scattering problem and obtain the total field at $y = b$, which is denoted by $\phi_{f_0}(x, b)$. Let A_{f_0}, B_{f_0} be the corresponding matrix and right-hand-side vector, but with the new data $\phi_{f_0}^{(m)}(b)$. Then we have an approximate equation

$$A_{f_0} F_0 = B_{f_0}. \tag{5.15}$$

Subtracting (5.15) from (4.12) yields

$$AF = A_{f_0} F_0 + B - B_{f_0}.$$

Inverting the above equation yields the updated Fourier coefficients:

$$F_1 = A^{\dagger} \left(A_{f_0} F_0 + B - B_{f_0} \right).$$

We then update the surface function as

$$f_1 = \mathrm{Re} \sum_{|m| \le N} F_1(m) e^{\mathrm{i}\alpha_m x}.$$

Repeating the above procedure gives the nonlinear correction scheme:

$$F_j = A^{\dagger} \left(A_{f_{j-1}} F_0 + B - B_{f_{j-1}} \right),$$
$$f_j = \mathrm{Re} \sum_{|m| \le N} F_j(m) e^{\mathrm{i}\alpha_m x},$$

$j = 0, 1, \ldots$, where $f_{-1} = A_{f_{-1}} = B_{f_{-1}} = 0$.

6. Numerical experiments

We generate the scattering data by solving the direct problem via the finite element method (FEM) with the perfectly matched layer (PML) technique [13]. A random noise of relative level δ is added to the data:

$$\phi_\delta(x, b) = \phi(x, b)(1 + \delta\, \mathrm{rand}),$$

where rand is a uniformly distributed random number in $[-1, 1]$.

We show a representative example. Let the exact surface function be given by $f(x) = \varepsilon g(x)$, where

$$g(x) = 0.5 \left(e^{\cos(2\pi(t-0.25)/\Lambda)} + e^{\cos(4\pi(t-0.25)/\Lambda)} - 1.2e \right).$$

The period of the surface is taken as $\Lambda = 1.0$ and the wavenumber in the air is taken as $\kappa = 2\pi$, which corresponds to a wavelength $\lambda = 1.0$. The deformation parameter is taken as $\varepsilon = 0.02$. The bottom of the slab is positioned at $y = h = 0.03\lambda$ and the top of the slab is at $y = b = 1.0\lambda$. Hence the slab is put in the near-field regime to the surface while the measured data is in the far-field regime. The noise level is taken as $\delta = 2\%$.

In Fig. 2(a)–(c), the reconstructed surface functions (dashed line) are plotted against the exact surface function (solid line) for $n = 1.0, 2.0, 4.0$, respectively. For $n = 1.0$, the slab is absent and the cut-off frequency is $N = 1$. Hence only the zeroth and first frequency modes may by reconstructed and the resolution is at most one wavelength. As n increases, more frequency modes are able to be recovered and the resolution increases to the subwavelength regime. Using the reconstruction in Fig. 2(c) as the initial guess, we apply

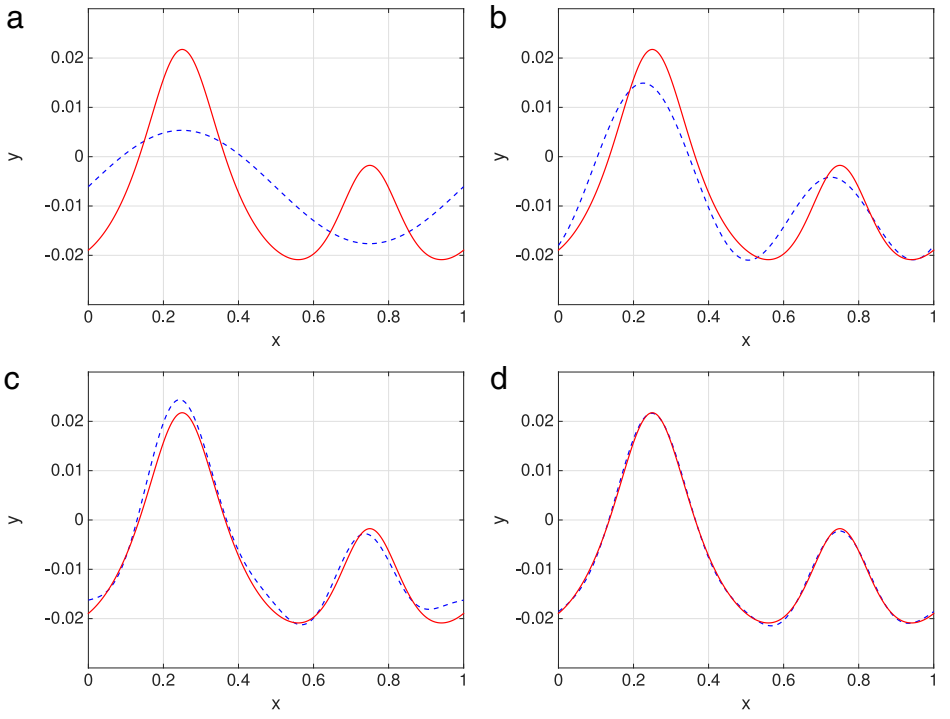

Fig. 2. (Color online) The reconstructed surface (dashed line) is plotted against the exact surface (solid line) for (a) $n = 1.0$; (b) $n = 2.0$; (c) $n = 4.0$; (d) $n = 4.0$ and after two iterations of nonlinear correction.

the nonlinear correction algorithm and obtain the result in Fig. 2(d) after two iterations. The reconstruction is almost perfect. Clearly, the algorithm is effective to increase the accuracy of the reconstruction.

7. Conclusion

Using the inverse diffraction grating problem, we demonstrated that super-resolution could be achieved stably by using the far-field data. Placing a slab of a homogeneous medium with a large index of refraction above the grating surface, we were allowed to convert more propagating wave components from the far-field to the near-field. Results show that the proposed method is effective to reconstruct grating surfaces with super-resolution. The method can be easily applied to other boundary conditions and problem geometry. We are extending the method to biperiodic structures where the full three-dimensional Maxwell equations should be considered.

Acknowledgments

The research of GB was supported in part by Key Project of the Major Research Plan of National Science Foundation China (NSFC) (No. 91130004); NSFC A3 Project (No. 11421110002); NSFC Tianyuan Project (No. 11426235). The research of PL was supported in part by National Science Foundation DMS-1151308.

References

[1] D. Courjon, Near-Field Microscopy and Near-Field Optics, Imperial College, 2003.
[2] C. Girard, A. Dereux, Near-field optics theories, Rep. Progr. Phys. 59 (1996) 657–699.
[3] N. García, M. Nieto-Vesperinas, Near-field optics inverse-scattering reconstruction of reflective surfaces, Opt. Lett. 24 (1993) 2090–2092.

[4] S. Carney, J. Schotland, Near-field tomography, MSRI Ser. Math. Appl. 47 (2003) 133–168.
[5] G. Bao, A unique theorem for an inverse problem in periodic diffractive optics, Inverse Problems 10 (1994) 335–340.
[6] G. Bao, D. Dobson, J.A. Cox, Mathematical studies in rigorous grating theory, J. Opt. Soc. Amer. A 12 (1995) 1029–1042.
[7] G. Bao, A. Friedman, Inverse problems for scattering by periodic structure, Arch. Ration. Mech. Anal. 132 (1995) 49–72.
[8] O. Bruno, F. Reitich, Numerical solution of diffraction problems: a method of variation of boundaries, J. Opt. Soc. Amer. A 10 (1993) 1168–1175.
[9] D.P. Nicholls, F. Reitich, Shape deformation in rough surface scattering: cancellation, conditioning, and convergence, J. Opt. Soc. Amer. A 21 (2004) 590–605.
[10] T. Cheng, P. Li, Y. Wang, Near-field imaging of perfectly conducting grating surfaces, J. Opt. Soc. Amer. A 30 (2013) 2473–2481.
[11] G. Bao, T. Cui, P. Li, Inverse diffraction grating of maxwell's equations in biperiodic structures, Opt. Express 22 (2014) 4799–4816.
[12] P. Li, Y. Wang, Y. Zhao, Inverse elastic surface scattering with near-field data, Inverse Problems 31 (2015) 035009.
[13] G. Bao, Z. Chen, H. Wu, Adaptive finite element method for diffraction gratings, J. Opt. Soc. Amer. A 22 (2005) 1106–1114.
[14] G. Bao, P. Li, H. Wu, A computational inverse diffraction grating problem, J. Opt. Soc. Amer. A 29 (2012) 394–399.
[15] G. Bao, P. Li, J. Lv, Numerical solution of an inverse dif- fraction grating problem from phaseless data, J. Opt. Soc. Amer. A 30 (2013) 293–299.